Phenomenological aspects of possible vacua of a neutrino flavor model *

Takuya Morozumi[1,2;1)] Hideaki Okane[1;2)] Hiroki Sakamoto[1;3)] Yusuke Shimizu[1;4)]
Kenta Takagi[1;5)] Hiroyuki Umeeda[3;6)]

[1] Graduate School of Science, Hiroshima University, Higashi-Hiroshima 739-8526, Japan
[2] Core of Research for the Energetic Universe, Hiroshima University, Higashi-Hiroshima 739-8526, Japan
[3] Graduate School of Science and Engineering, Shimane University, Matsue 690-8504, Japan

Abstract: We discuss a supersymmetric model with discrete flavor symmetry $A_4 \times Z_3$. The additional scalar fields which contribute masses of leptons in the Yukawa terms are introduced in this model. We analyze their scalar potential and find that they have various vacuum structures. We show the relations among 24 different vacua and classify them into two types. We derive expressions of the lepton mixing angles, Dirac CP violating phase and Majorana phases for the two types. The model parameters which are allowed by the experimental data of the lepton mixing angles are different for each type. We also study the constraints on the model parameters which are related to Majorana phases. The different allowed regions of the model parameters for the two types are shown numerically for a given region of two combinations of the CP violating phases.

Keywords: flavor symmetry, non-Abelian discrete group, neutrino flavor model

PACS: 14.60.Pq, 14.60.St **DOI:** 10.1088/1674-1137/42/2/023102

1 Introduction

Although all the elementary particles in the standard model (SM) have now been discovered, with the discovery of the Higgs boson, there still exist phenomena which cannot be explained in the framework of the SM. One of these is the neutrino oscillation phenomenon, which implies two non-zero neutrino mass squared differences and two large lepton mixing angles. In order to explain this, many authors propose a neutrino flavor model with non-Abelian discrete flavor symmetry in the lepton sector (for reviews see [1–4]). Even before the discovery of the non-zero θ_{13} [5–7], a few authors suggested a tiny mixing angle θ_{13} based on non-Abelian discrete flavor symmetry [8]. Recent results from the T2K and NOνA experiments [9, 10] imply CP violation through the Dirac CP phase. They studied electron neutrino appearance in a muon neutrino beam. The Majorana phases are also sources of the CP violating phases if neutrinos are Majorana particles. The KamLAND-Zen experiment [11] is searching for neutrinoless double beta ($0\nu\beta\beta$) decay to check the Majorana nature of neutrinos. Therefore, it is important to predict not only mixing angles but also CP phases with the non-Abelian discrete flavor model.

The non-Abelian discrete flavor symmetry can easily explain large lepton mixing angles, e. g. tri-bimaximal mixing (TBM) [12, 13], which is a simple framework for the lepton mixing angles. Indeed, Altarelli and Feruglio (AF) proposed a simple flavor model and predicted TBM by using A_4 discrete flavor symmetry [14, 15]. They introduced $SU(2)$ gauge singlet scalar fields, so-called "flavons", and derived the TBM in the lepton sector. The non-zero θ_{13} can be realized by another A_4 non-trivial singlet flavon [8] in addition to the flavons introduced by AF. The origin of non-vanishing θ_{13} is related to a new contribution to the mass matrices. Matrices which have the same structure as that in Ref. [8] also appear in extra-dimensional models with the S_3 and S_4

Received 3 October 2017, Published online 12 January 2018

∗ Supported by JSPS KAKENHI Grant Number JP17K05418 (T.M.). This work is also supported in part by Grants-in-Aid for Scientific Research [No. 16J05332 (Y.S.), Nos. 24540272, 26247038, 15H01037, 16H00871, and 16H02189 (H.U.)] from the Ministry of Education, Culture, Sports, Science and Technology in Japan. H.O. is also supported by Hiroshima Univ. Alumni Association

1) E-mail: morozumi@hiroshima-u.ac.jp
2) E-mail: hideaki-ookane@hiroshima-u.ac.jp
3) E-mail: h-sakamoto@hiroshima-u.ac.jp
4) E-mail: yu-shimizu@hiroshima-u.ac.jp
5) E-mail: takagi-kenta@hiroshima-u.ac.jp
6) E-mail: umeeda@riko.shimane-u.ac.jp

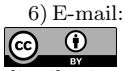

flavor symmetries [16, 17]. The $\Delta(27)$ model also includes these matrices [18].

In this paper, we study phenomenological aspects of a supersymmetric model with $A_4\times Z_3$ symmetries. The three generations of the left-handed leptons are expressed as the A_4 triplet, $l=(l_e,l_\mu,l_\tau)$, while the right-handed charged leptons e_R, μ_R, and τ_R are A_4 singlets denoted as $\mathbf{1}$, $\mathbf{1}''$, and $\mathbf{1}'$ respectively. Three right-handed neutrinos are also described as the triplet of A_4. We introduce the $SU(2)$ gauge singlet flavons of A_4 triplets, $\phi_T=(\phi_{T1},\phi_{T2},\phi_{T3})$ and $\phi_S=(\phi_{S1},\phi_{S2},\phi_{S3})$. In addition, ξ and ξ' are also introduced as the $SU(2)$ gauge singlet flavons with the two kinds of singlet representations of A_4, $\mathbf{1}$ and $\mathbf{1}'$ respectively.

We focus on the vacuum structure of the flavor model. The scalar sectors of this model consist of many flavons in addition to the SM Higgs boson. Then, we analyze the scalar potential and show the 24 different sets of VEVs which come from 24 combinations of 4 (6) possible VEVs of the flavon ϕ_T (ϕ_S). The 24 different vacua are classified into two types which are not related to each other under the transformations A_4. Therefore, we expect that the two types of vacua have different expressions for the physical observables in terms of the model parameters such as Yukawa couplings. We ask the following question: whether these different vacua are physically distinct from each other. The purpose of this paper is to clarify the differences and relations among the VEVs and their physical consequences. In particular, we investigate the mixing angles, CP violating phase, and effective mass for neutrinoless double beta ($0\nu\beta\beta$) decay.

This paper is organized as follows. In Section 2, we introduce the supersymmetric model with $A_4\times Z_3$ symmetry. In Section 3, we study the classification of vacua and derive the formulae for the mixing angles and CP phases. In Section 4, we discuss the phenomenological aspects for mixing angles and CP violating phases. The numerical analyses for the effective mass of $0\nu\beta\beta$ decay are presented. Section 5 is devoted to a summary. In Appendix , we show the multiplication rule of the A_4 group.

2 Supersymmetric model with $A_4\times Z_3$ symmetry

In this section, we introduce a supersymmetric model with $A_4\times Z_3$ symmetry. We analyze the scalar potential and derive the mass matrices of the lepton sector.

2.1 Model

We introduce three heavy right-handed Majorana neutrinos. The leptons and scalars in our model are listed in Table 1.

Table 1. The representations of $SU(2)_L$ and A_4, and the charge assignment of Z_3 and $U(1)_R$ for leptons and scalars: $l_{e,\mu,\tau}$, $\{e,\mu,\tau\}_R$, $\{\nu_e,\nu_\mu,\mu_\tau\}_R$, and $h_{u,d}$ denote left-handed leptons, right-handed charged leptons, right-handed neutrinos, and Higgs fields, respectively. The other scalars are gauge singlet flavons and denoted as ϕ_T, ϕ_S, ξ, and ξ'. ω is the Z_3 charge and stands for $e^{2\pi i/3}$.

	$l=\begin{pmatrix}l_e\\l_\mu\\l_\tau\end{pmatrix}$	e_R	μ_R	τ_R	$\nu_R=\begin{pmatrix}\nu_{eR}\\\nu_{\mu R}\\\nu_{\tau R}\end{pmatrix}$	$h_{u,d}$	$\phi_T=\begin{pmatrix}\phi_{T1}\\\phi_{T2}\\\phi_{T3}\end{pmatrix}$	$\phi_S=\begin{pmatrix}\phi_{S1}\\\phi_{S2}\\\phi_{S3}\end{pmatrix}$	ξ	ξ'
$SU(2)_L$	2	1	1	1	1	2	1	1	1	1
A_4	3	1	$1''$	$1'$	3	1	3	3	1	$1'$
Z_3	ω	ω^2	ω^2	ω^2	ω^2	1	1	ω^2	ω^2	ω^2
$U(1)_R$	1	1	1	1	1	0	0	0	0	0

The superpotential of Yukawa interactions is

$$w_Y=w_l+w_D+w_R, \tag{1}$$

where w_l,w_D and w_R are Yukawa interactions for charged lepton, Dirac neutrino and Majorana neutrino sectors respectively:

$$\begin{aligned}w_l=&y_e(\phi_T l)_{\mathbf{1}}e_R h_d/\Lambda+y_\mu(\phi_T l)_{\mathbf{1}'}\mu_R h_d/\Lambda\\&+y_\tau(\phi_T l)_{\mathbf{1}''}\tau_R h_d/\Lambda+\text{h.c.},\end{aligned} \tag{2}$$

$$w_D=y_D(l\nu_R)_{\mathbf{1}}h_u+\text{h.c.}, \tag{3}$$

$$w_R=y_{\phi_S}\phi_S(\nu_R\nu_R)_{\mathbf{3}}+y_\xi\xi(\nu_R\nu_R)_{\mathbf{1}}+y_{\xi'}\xi'(\nu_R\nu_R)_{\mathbf{1}''}+\text{h.c.}, \tag{4}$$

where the lower indices denote A_4 representations. Moreover, the y's and Λ denote the Yukawa coupling constants and cut-off scale respectively. The multiplication rule for A_4 representations is shown in Appendix A.

In order to obtain the mass matrices of these leptons, we analyze the following superpotential of the scalar fields:

$$w_d\equiv w_d^T+w_d^S, \tag{5}$$

where

$$w_d^T=-M(\phi_0^T\phi_T)_{\mathbf{1}}+g\phi_0^T(\phi_T\phi_T)_{\mathbf{3}}, \tag{6}$$

$$\begin{aligned}w_d^S=&g_1\phi_0^S(\phi_S\phi_S)_{\mathbf{3}}+g_2(\phi_0^S\phi_S)_{\mathbf{1}}\xi+g_2'(\phi_0^S\phi_S)_{\mathbf{1}''}\xi'\\&+g_3(\phi_S\phi_S)_{\mathbf{1}}\xi_0-g_4\xi_0\xi\xi.\end{aligned} \tag{7}$$

Table 2. The driving fields and their representations and charge assignment.

	$\phi_0^T=\begin{pmatrix}\phi_{01}^T\\ \phi_{02}^T\\ \phi_{03}^T\end{pmatrix}$	$\phi_0^S=\begin{pmatrix}\phi_{01}^S\\ \phi_{02}^S\\ \phi_{03}^S\end{pmatrix}$	ξ_0
$SU(2)$	1	1	1
A_4	3	3	1
Z_3	1	ω^2	ω^2
$U(1)_R$	2	2	2

We have introduced the additional $SU(2)$ gauge singlet fields, ϕ_0^T, ϕ_0^S and ξ_0, which are called *"driving fields"*. The charge assignments of these fields are summarized in Table 2.

2.2 Potential analysis

In this subsection, we derive the VEVs for the scalar fields $\phi_T,\phi_S,\xi,\xi',\phi_0^T,\phi_0^S,\xi_0$. One can derive the scalar potential from the superpotentials in Eqs. (6) and (7) as

$$V=V_T+V_S, \tag{8}$$

where

$$\begin{aligned}V_T=\sum_X\left|\frac{\partial w_d^T}{\partial X}\right|^2=&\left|-M\phi_{T1}+\frac{2}{3}g(\phi_{T1}^2-\phi_{T2}\phi_{T3})\right|^2+\left|-M\phi_{T3}+\frac{2}{3}g(\phi_{T2}^2-\phi_{T3}\phi_{T1})\right|^2+\left|-M\phi_{T2}+\frac{2}{3}g(\phi_{T3}^2-\phi_{T1}\phi_{T2})\right|^2\\&+\left|-M\phi_{01}^T+\frac{2}{3}g(2\phi_{01}^T\phi_{T1}-\phi_{03}^T\phi_{T2}-\phi_{02}^T\phi_{T3})\right|^2+\left|-M\phi_{03}^T+\frac{2}{3}g(2\phi_{02}^T\phi_{T2}-\phi_{01}^T\phi_{T3}-\phi_{03}^T\phi_{T1})\right|^2\\&+\left|-M\phi_{02}^T+\frac{2}{3}g(2\phi_{03}^T\phi_{T3}-\phi_{02}^T\phi_{T1}-\phi_{01}^T\phi_{T2})\right|^2,\end{aligned} \tag{9}$$

and

$$\begin{aligned}V_S=\sum_Y\left|\frac{\partial w_d^S}{\partial Y}\right|^2=&\left|\frac{2}{3}g_1(\phi_{S1}^2-\phi_{S2}\phi_{S3})-g_2\phi_{S1}\xi+g_2'\phi_{S3}\xi'\right|^2+\left|\frac{2}{3}g_1(\phi_{S2}^2-\phi_{S3}\phi_{S1})-g_2\phi_{S3}\xi+g_2'\phi_{S2}\xi'\right|^2\\&+\left|\frac{2}{3}g_1(\phi_{S3}^2-\phi_{S1}\phi_{S2})-g_2\phi_{S2}\xi+g_2'\phi_{S1}\xi'\right|^2\\&+\left|\frac{2}{3}g_1(2\phi_{01}^S\phi_{S1}-\phi_{03}^S\phi_{S2}-\phi_{02}^S\phi_{S3})-g_2\phi_{01}^S\xi+g_2'\phi_{03}^S\xi'+2g_3\phi_{S1}\xi_0\right|^2\\&+\left|\frac{2}{3}g_1(2\phi_{02}^S\phi_{S2}-\phi_{01}^S\phi_{S3}-\phi_{03}^S\phi_{S1})-g_2\phi_{03}^S\xi+g_2'\phi_{02}^S\xi'+2g_3\phi_{S3}\xi_0\right|^2\\&+\left|\frac{2}{3}g_1(2\phi_{03}^S\phi_{S3}-\phi_{02}^S\phi_{S1}-\phi_{01}^S\phi_{S2})-g_2\phi_{02}^S\xi+g_2'\phi_{01}^S\xi'+2g_3\phi_{S2}\xi_0\right|^2\\&+\left|-g_2(\phi_{01}^S\phi_{S1}+\phi_{03}^S\phi_{S2}+\phi_{02}^S\phi_{S3})-2g_4\xi\xi_0\right|^2+\left|g_2'(\phi_{02}^S\phi_{S2}+\phi_{01}^S\phi_{S3}+\phi_{03}^S\phi_{S1})\right|^2\\&+\left|g_3(\phi_{s1}^2+2\phi_{S2}\phi_{S3})-g_4\xi^2\right|^2.\end{aligned} \tag{10}$$

The sum for X,Y runs over all the scalar fields:

$$X=\{\phi_{T1},\phi_{T2},\phi_{T3},\phi_{01}^T,\phi_{02}^T,\phi_{03}^T\}\ ,$$

$$Y=\{\phi_{S1},\phi_{S2},\phi_{S3},\phi_{01}^S,\phi_{02}^S,\phi_{03}^S,\xi,\xi',\xi_0\}.$$

The scalar potential V is minimized at $V=V_T=V_S=0$. There are several solutions for the minimization condition. We obtain sets of solutions denoted as η_m and $\lambda_n^{\pm}$ (m=1-4, n=1-3), where η_m and $\lambda_n^{\pm}$ are the solutions of $V_T=0$ and $V_S=0$ respectively. Hereafter, we call them the set of VEV alignments and show them explicitly as follows:

$$\eta_1\equiv\left\{\langle\phi_T\rangle=v_T\begin{pmatrix}1\\0\\0\end{pmatrix},\ \langle\phi_0^T\rangle=\begin{pmatrix}0\\0\\0\end{pmatrix}\right\}, \tag{11}$$

$$\eta_2\equiv\left\{\langle\phi_T\rangle=\frac{v_T}{3}\begin{pmatrix}-1\\2\\2\end{pmatrix},\ \langle\phi_0^T\rangle=\begin{pmatrix}0\\0\\0\end{pmatrix}\right\}, \tag{12}$$

$$\eta_3\equiv\left\{\langle\phi_T\rangle=\frac{v_T}{3}\begin{pmatrix}-1\\2\omega\\2\omega^2\end{pmatrix},\ \langle\phi_0^T\rangle=\begin{pmatrix}0\\0\\0\end{pmatrix}\right\}, \tag{13}$$

$$\eta_4\equiv\left\{\langle\phi_T\rangle=\frac{v_T}{3}\begin{pmatrix}-1\\2\omega^2\\2\omega\end{pmatrix},\ \langle\phi_0^T\rangle=\begin{pmatrix}0\\0\\0\end{pmatrix}\right\}, \tag{14}$$

$$\lambda_1^{\pm}\equiv\left\{\langle\phi_S\rangle=\pm v_S\begin{pmatrix}1\\1\\1\end{pmatrix},\ \langle\xi'\rangle=u',\ \langle\phi_0^S\rangle=\begin{pmatrix}0\\0\\0\end{pmatrix}\right\},\quad(15)$$

$$\lambda_2^{\pm}\equiv\left\{\langle\phi_S\rangle=\pm v_S\begin{pmatrix}1\\\omega\\\omega^2\end{pmatrix},\ \langle\xi'\rangle=\omega u',\ \langle\phi_0^S\rangle=\begin{pmatrix}0\\0\\0\end{pmatrix}\right\},\quad(16)$$

$$\lambda_3^{\pm}\equiv\left\{\langle\phi_S\rangle=\pm v_S\begin{pmatrix}1\\\omega^2\\\omega\end{pmatrix},\ \langle\xi'\rangle=\omega^2 u',\ \langle\phi_0^S\rangle=\begin{pmatrix}0\\0\\0\end{pmatrix}\right\},\quad(17)$$

where $v_T=\frac{3M}{2g}$, $v_S=\sqrt{\frac{g_4}{3g_3}}u$, $u'=\frac{g_2}{g_2'}u$ and u is the VEV of ξ, $\langle\xi\rangle=u$[1]. The superscript of $\lambda^{\pm}$ denotes the overall sign of the VEV $\langle\phi_S\rangle$. In total, we obtain 24 sets of vacua, since there are four sets of alignment for η_m and six sets for $\lambda_n^{\pm}$.

2.3 Mass matrix for charged leptons and neutrinos

We derive charged lepton mass matrices and neutrino mass matrices from the Yukawa interactions in Eqs. (2), (3), and (4). These matrices are expressed in various forms corresponding to the VEV alignments. The charged lepton mass matrices $M_l{}^{(m)}$ for Eqs. (11)–(14) are

$$M_l{}^{(1)}=\frac{v_d v_T}{\Lambda}\begin{pmatrix}y_e&0&0\\0&y_\mu&0\\0&0&y_\tau\end{pmatrix},\quad(18)$$

$$M_l{}^{(2)}=\frac{v_d v_T}{3\Lambda}\begin{pmatrix}-y_e&2y_\mu&2y_\tau\\2y_e&-y_\mu&2y_\tau\\2y_e&2y_\mu&-y_\tau\end{pmatrix}=SM_l{}^{(1)},\quad(19)$$

$$M_l{}^{(3)}=\frac{v_d v_T}{3\Lambda}\begin{pmatrix}-y_e&2\omega y_\mu&2\omega^2 y_\tau\\2\omega^2 y_e&-y_\mu&2\omega y_\tau\\2\omega y_e&2\omega^2 y_\mu&-y_\tau\end{pmatrix}=T^\dagger STM_l{}^{(1)},\quad(20)$$

$$M_l{}^{(4)}=\frac{v_d v_T}{3\Lambda}\begin{pmatrix}-y_e&2\omega^2 y_\mu&2\omega y_\tau\\2\omega y_e&-y_\mu&2\omega^2 y_\tau\\2\omega^2 y_e&2\omega y_\mu&-y_\tau\end{pmatrix}=TST^\dagger M_l{}^{(1)},\quad(21)$$

respectively, where the matrices S and T are

$$S=\frac{1}{3}\begin{pmatrix}-1&2&2\\2&-1&2\\2&2&-1\end{pmatrix},\quad T=\begin{pmatrix}1&0&0\\0&\omega&0\\0&0&\omega^2\end{pmatrix}.\quad(22)$$

The Dirac mass matrix for neutrinos obtained from Eq. (3) is

$$M_D=y_D v_u\begin{pmatrix}1&0&0\\0&0&1\\0&1&0\end{pmatrix}.\quad(23)$$

It is noted that the Dirac mass matrix is determined independently of the VEV alignments. The Majorana mass matrices $M_R^{(n)\pm}$ for the corresponding set of solutions Eqs. (15)–(17) are given as follows:

$$M_R^{(1)\pm}=\pm\frac{1}{3}y_{\phi_S}v_S\begin{pmatrix}2&-1&-1\\-1&2&-1\\-1&-1&2\end{pmatrix}+y_\xi u\begin{pmatrix}1&0&0\\0&0&1\\0&1&0\end{pmatrix}+y_{\xi'}u'\begin{pmatrix}0&0&1\\0&1&0\\1&0&0\end{pmatrix},\quad(24)$$

$$M_R^{(2)\pm}=\pm\frac{1}{3}y_{\phi_S}v_S\begin{pmatrix}2&-\omega^2&-\omega\\-\omega^2&2\omega&-1\\-\omega&-1&2\omega^2\end{pmatrix}+y_\xi u\begin{pmatrix}1&0&0\\0&0&1\\0&1&0\end{pmatrix}+\omega y_{\xi'}u'\begin{pmatrix}0&0&1\\0&1&0\\1&0&0\end{pmatrix}=T^\dagger M_R^{(1)\pm}T^\dagger,\quad(25)$$

$$M_R^{(3)\pm}=\pm\frac{1}{3}y_{\phi_S}v_S\begin{pmatrix}2&-\omega&-\omega^2\\-\omega&2\omega^2&-1\\-\omega^2&-1&2\omega\end{pmatrix}+y_\xi u\begin{pmatrix}1&0&0\\0&0&1\\0&1&0\end{pmatrix}+\omega^2 y_{\xi'}u'\begin{pmatrix}0&0&1\\0&1&0\\1&0&0\end{pmatrix}=TM_R^{(1)\pm}T.\quad(26)$$

In order to generate the light neutrino mass matrices, we adopt the seesaw mechanism [19–21]. The effective neutrino mass matrices are given by the well-known formula, $M_\nu=-M_D M_R^{-1}M_D^{\rm T}$, through the seesaw mechanism. We obtain the 6 different effective neutrino mass

1) There are still other solutions for $V=0$, including the trivial solution which makes all the VEVs vanish. It leads to the vanishing of all the lepton masses and mixing angles. In addition to the trivial solution, there are solutions with non-zero VEVs of the driving fields. This case leads to the breakdown of $U(1)_R$ symmetry. In this paper, we only discuss the vacua where $U(1)_R$ symmetry is conserved.

matrices from Eqs. (23)-(26) as follows:

$$M_\nu^{(1)\pm}=\pm a\begin{pmatrix}1&0&0\\0&1&0\\0&0&1\end{pmatrix}+b^\pm\begin{pmatrix}1&1&1\\1&1&1\\1&1&1\end{pmatrix}+c\begin{pmatrix}1&0&0\\0&0&1\\0&1&0\end{pmatrix}+d\begin{pmatrix}0&0&1\\0&1&0\\1&0&0\end{pmatrix}, \quad (27)$$

$$M_\nu^{(2)\pm}=T^\dagger M_\nu^{(1)\pm}T^\dagger, \quad (28)$$

$$M_\nu^{(3)\pm}=TM_\nu^{(1)\pm}T, \quad (29)$$

where

$$\begin{aligned}&a=ky_{\phi_S}v_S,\\&c=k(y_{\xi'}u'-y_\xi u),\\&d=ky_{\xi'}u',\\&b^\pm=\mp\frac{a}{3}+\frac{a^2}{2d-c}\left(\frac{1}{3}-\frac{d^2}{a^2}\right),\\&k=\frac{{y_D}^2{v_u}^2}{y_\xi^2u^2+y_{\xi'}^2u'^2-(y_{\phi_S}^2v_S^2+y_\xi uy'_\xi u')}.\end{aligned}$$

3 Classification of vacua and PMNS mixing matrix

In this section, we classify the 24 different vacua and derive the lepton mixing matrix $U_{\rm PMNS}$, called the *Pontecorvo-Maki-Nakagawa-Sakata* (PMNS) mixing matrix. In order to classify the vacua, we discuss the relations among the VEV alignments with the transformations of A_4. We show that the 24 vacua are classified into two types in the following subsection. Then, one finds the two different PMNS matrices with diagonalizing matrices for the charged lepton and effective neutrino mass matrices Eqs. (18)–(21), and (27)–(29).

3.1 Relations among sets of VEV alignments

The generators of A_4 are expressed as the following forms for the representations $\mathbf{1}$,$\mathbf{1}'$,$\mathbf{1}''$ and $\mathbf{3}$,

$$S(\mathbf{1})=S(\mathbf{1}')=S(\mathbf{1}'')=1\ ,\quad S(\mathbf{3})=\frac{1}{3}\begin{pmatrix}-1&2&2\\2&-1&2\\2&2&-1\end{pmatrix}, \quad (30)$$

$$T(\mathbf{1})=1,\ T(\mathbf{1}')=\omega,\ T(\mathbf{1}'')=\omega^2\ ,\quad T(\mathbf{3})=\begin{pmatrix}1&0&0\\0&\omega&0\\0&0&\omega^2\end{pmatrix}. \quad (31)$$

The sets of VEV alignment η_m,$\lambda_n^\pm$ are associated through the transformations of these generators. As an example, we show the T transformation on λ_1^+:

$$T[\lambda_1^+]\equiv\left\{\langle\phi_S\rangle=T(\mathbf{3})v_S\begin{pmatrix}1\\1\\1\end{pmatrix},\langle\xi'\rangle=T(\mathbf{1}')u',\langle\phi_0^S\rangle=T(\mathbf{3})\begin{pmatrix}0\\0\\0\end{pmatrix}\right\}=\left\{\langle\phi_S\rangle=v_S\begin{pmatrix}1\\\omega\\\omega^2\end{pmatrix},\langle\xi'\rangle=\omega u',\ \langle\phi_0^S\rangle=\begin{pmatrix}0\\0\\0\end{pmatrix}\right\}=\lambda_2^+. \quad (32)$$

The S and T transformations on all the sets of the VEV alignment are summarized in Fig. 1. Some transformations preserve the VEVs of either η_m or $\lambda_n^\pm$. These vacua have Z_3 or Z_2 symmetries as the residual symmetries of A_4 respectively. For the VEVs described as η_m, they are invariant under the following transformation,

$$\begin{aligned}&T[\eta_1]=T^{-1}[\eta_1]=\eta_1\ ,\quad TST[\eta_2]=(TST)^{-1}[\eta_2]=\eta_2\ ,\\&ST[\eta_3]=(ST)^{-1}[\eta_3]=\eta_3\ ,\quad TS[\eta_4]=(TS)^{-1}[\eta_4]=\eta_4\ .\end{aligned} \quad (33)$$

It is easy to confirm that such transformations correspond to Z_3 symmetries:

$$T^3=(TST)^3=(ST)^3=(TS)^3=1. \quad (34)$$

Each $\lambda_n^\pm$ has Z_2 symmetry as follows:

$$S[\lambda_1^\pm]=\lambda_1^\pm\ ,\quad TST^2[\lambda_2^\pm]=\lambda_2^\pm\ ,\quad T^2ST[\lambda_3^\pm]=\lambda_3^\pm, \quad (35)$$

where

$$S^2=(TST^2)^2=(T^2ST)^2=1. \quad (36)$$

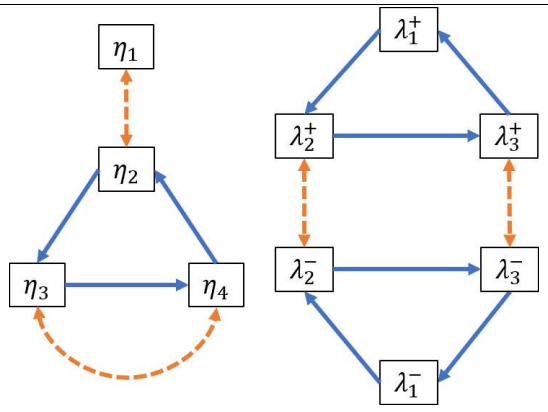

Fig. 1. (color online) Map of the transitions among the VEV alignments under the transformations S and T: The solid arrow corresponds to the transition due to T transformation and the dashed two headed arrow shows the transition due to S transformation. In the map, η_1 is invariant under T transformation while $\lambda_1^\pm$ are invariant under S transformation.

3.2 Classification of 24 vacua

In this subsection, we show the relations among the 24 different Lagrangians derived from the 24 different combinations of VEV alignments in Eqs. (11)–(17). We find the two sets of 12 equivalent Lagrangians with the appropriate field redefinitions. Then, the 24 Lagrangians are classified into two types. For simplicity, we write the Lagrangian of this model in a short form:

$$\mathcal{L}(\psi,\phi_1,\phi_2), \tag{37}$$

where ψ represents the fermion fields such as l and ν_R. ϕ_1 and ϕ_2 represent the scalar fields, which should have their VEVs written as η_m and $\lambda_n^{\pm}$ respectively. We write the Lagrangian in the broken phase for the VEV alignment $(\eta_m,\ \lambda_n^{\pm})$ with fluctuations h_1 and h_2 as

$$\mathcal{L}^{\pm}_{mn}(\psi,h_1,h_2)\equiv\mathcal{L}(\psi,\eta_m+h_1,\lambda_n^{\pm}+h_2). \tag{38}$$

Then, we prove the following equation:

$$\mathcal{L}(\psi',\eta_m+h_1',\lambda_n^{\pm}+h_2')=\mathcal{L}(\psi,G^{-1}\eta_m+h_1,G^{-1}\lambda_n^{\pm}+h_2), \tag{39}$$

where G denotes the transformation composed of S and T in Eqs. (30) and (31). There are 12 independent transformations including the identity element:

$$\begin{aligned} &G;\{e,\ T,\ T^2,\ S,\ TS,\ T^2S,\ ST,\ ST^2,\ T^2ST,\\ &\quad TST,\ TST^2,\ T^2ST^2\}. \end{aligned} \tag{40}$$

The redefined fields are written as follows,

$$\psi'=G\psi\ ,\quad h_i'=Gh_i\quad (i=1,2). \tag{41}$$

The right-hand side of Eq. (39) corresponds to the Lagrangian for the vacuum $(G^{-1}\eta_m,G^{-1}\lambda_n^{\pm})$ while the left-hand side is the Lagrangian for the vacuum $(\eta_m,\lambda_n^{\pm})$ in terms of the redefined fields. In the symmetric phase, the Lagrangian $\mathcal{L}(\psi,\phi_1,\phi_2)$ is invariant under the G transformation,

$$\mathcal{L}(G\psi,G\phi_1,G\phi_2)=\mathcal{L}(\psi,\phi_1,\phi_2). \tag{42}$$

One obtains the following equation from Eq. (42) for the vacuum $(G^{-1}\eta_m,G^{-1}\lambda_n^{\pm})$,

$$\mathcal{L}(G\psi,\eta_m+Gh_1,\lambda_n^{\pm}+Gh_2)=\mathcal{L}(\psi,G^{-1}\eta_m+h_1,G^{-1}\lambda_n^{\pm}+h_2). \tag{43}$$

Finally, one obtains the relation Eq. (39) by applying the field definition Eq. (41) to the left-hand side of Eq. (43). The relation Eq. (39) implies the equality of the Lagrangians for the two vacua $(\eta_m,\lambda_n^{\pm})$ and $(G^{-1}\eta_m,G^{-1}\lambda_n^{\pm})$.

Here, we briefly show how to find the equivalent vacua with Fig. 1. For example, let us consider the T transformation in terms of the vacuum of (η_1,λ_1^+). One finds that η_1 is invariant and λ_1^+ transfers to λ_2^+ under the T transformation. Therefore, $\mathcal{L}_{11}^+$ and $\mathcal{L}_{12}^+$ are equivalent. One can find 12 equivalent vacua by applying 12 independent transformations in Eq. (40) to the vacuum (η_1,λ_1^+). Then, we classify the 24 Lagrangians into two types:

Type I;
$$\{\mathcal{L}_{11}^+,\mathcal{L}_{12}^+,\mathcal{L}_{13}^+,\mathcal{L}_{21}^+,\mathcal{L}_{32}^+,\mathcal{L}_{43}^+,\mathcal{L}_{22}^-,\mathcal{L}_{23}^-,\mathcal{L}_{31}^-,\mathcal{L}_{33}^-,\mathcal{L}_{41}^-,\mathcal{L}_{42}^-\}, \tag{44}$$

Type II;
$$\{\mathcal{L}_{11}^-,\mathcal{L}_{12}^-,\mathcal{L}_{13}^-,\mathcal{L}_{21}^-,\mathcal{L}_{32}^-,\mathcal{L}_{43}^-,\mathcal{L}_{22}^+,\mathcal{L}_{23}^+,\mathcal{L}_{31}^+,\mathcal{L}_{33}^+,\mathcal{L}_{41}^+,\mathcal{L}_{42}^+\}. \tag{45}$$

Type I and type II are disconnected because of the absence of a transformation which relates one type to the other. Since all the Lagrangians which belong to the same type lead to the same physical consequences, we consider only $\mathcal{L}_{11}^+$ and $\mathcal{L}_{11}^-$ as the representatives of their types:

$$\mathcal{L}^{\rm I}\equiv\mathcal{L}_{11}^+\ ,\quad \mathcal{L}^{\rm II}\equiv\mathcal{L}_{11}^-. \tag{46}$$

We also define the representative mass matrices for charged leptons and neutrinos as

$$M_l\equiv M_l^{(1)}\ ,\quad M_\nu^{\rm I}\equiv M_\nu^{(1)^+}\ ,\quad M_\nu^{\rm II}\equiv M_\nu^{(1)^-}. \tag{47}$$

It is noted that the charged lepton mass matrix $M_l^{(1)}$ is diagonal.

3.3 PMNS matrices for two types

In this subsection, we construct the PMNS matrices for the two types, $\mathcal{L}^{\rm I}$ and $\mathcal{L}^{\rm II}$. Since the charged lepton mass matrix M_l is diagonal, the PMNS matrix is determined so that it diagonalizes the neutrino mass matrices in Eq. (27):

$$\begin{aligned}(U_{\rm PMNS}^{\rm I})^\dagger M_\nu^{\rm I}(U_{\rm PMNS}^{\rm I})^*&=(U_{\rm PMNS}^{\rm II})^\dagger M_\nu^{\rm II}(U_{\rm PMNS}^{\rm II})^*\\ &=\begin{pmatrix} m_1 & & \\ & m_2 & \\ & & m_3\end{pmatrix},\end{aligned} \tag{48}$$

where the left-handed neutrino masses m_1,m_2 and m_3 are positive. The PMNS matrices are expressed as the following forms for the two types:

$$U_{\rm PMNS}^{\rm I}=U_{\rm TBM}U_{13}(\theta,\sigma)\begin{pmatrix} e^{i\phi_1} & & \\ & e^{i\phi_2} & \\ & & e^{i\phi_3}\end{pmatrix}, \tag{49}$$

$$\begin{aligned}U_{\rm PMNS}^{\rm II}&=U_{\rm TBM}\begin{pmatrix} & & -i\\ 1 & & \\ & i & \end{pmatrix}U_{13}(\theta,\sigma)\begin{pmatrix} e^{i\phi_1} & & \\ & e^{i\phi_2} & \\ & & e^{i\phi_3}\end{pmatrix},\\ &=U_{\rm TBM}U_{13}^*\left(\theta+\frac{\pi}{2},\sigma\right)\begin{pmatrix} -ie^{i(\phi_1+\sigma)} & & \\ & e^{i\phi_2} & \\ & & -ie^{i(\phi_3-\sigma)}\end{pmatrix}.\end{aligned} \tag{50}$$

The unitary matrix $U_{\rm TBM}$ is the tri-bimaximal mixing matrix and $U_{13}(\theta,\sigma)$ denotes the unitary rotation matrix:

$$U_{\rm TBM}=\begin{pmatrix} 2/\sqrt{6} & 1/\sqrt{3} & 0 \\ -1/\sqrt{6} & 1/\sqrt{3} & -1/\sqrt{2} \\ -1/\sqrt{6} & 1/\sqrt{3} & 1/\sqrt{2} \end{pmatrix}, \tag{51}$$

$$U_{13}(\theta,\sigma)=\begin{pmatrix} \cos\theta & 0 & {\rm e}^{-{\rm i}\sigma}\sin\theta \\ 0 & 1 & 0 \\ -{\rm e}^{{\rm i}\sigma}\sin\theta & 0 & \cos\theta \end{pmatrix}. \tag{52}$$

We have introduced the parameters θ,σ and ϕ_i (i=1,2,3). They are written in terms of the complex parameters of the neutrino mass matrix, a,b,c and d, in Eq. (27)[1]. In the rest of this subsection, we derive the explicit forms of the parameters θ,σ and ϕ_i in terms of the model parameters a,b,c and d. In the first step, one rotates $M_\nu M_\nu^\dagger$ with the tri-bimaximal mixing matrix.

$$U_{\rm TBM}^\dagger M_\nu^{\rm I}(M_\nu^{\rm I})^\dagger U_{\rm TBM}=\begin{pmatrix} A & 0 & B \\ 0 & C & 0 \\ B^* & 0 & D \end{pmatrix}, \tag{53}$$

$$U_{\rm TBM}^\dagger M_\nu^{\rm II}(M_\nu^{\rm II})^\dagger U_{\rm TBM}=\begin{pmatrix} D & 0 & -B^* \\ 0 & C & 0 \\ -B & 0 & A \end{pmatrix}. \tag{54}$$

where

$$A=\left|a+c-\frac{d}{2}\right|^2+\left|\frac{\sqrt{3}}{2}d\right|^2, \tag{55}$$

$$B=\left(a+c-\frac{d}{2}\right)\frac{\sqrt{3}}{2}d^*+\frac{\sqrt{3}}{2}d\left(a-c+\frac{d}{2}\right)^*\equiv|B|{\rm e}^{{\rm i}\varphi_B}, \tag{56}$$

$$C=\left|\frac{a^2-(c^2-cd+d^2)}{2d-c}\right|^2, \tag{57}$$

$$D=\left|a-c+\frac{d}{2}\right|^2+\left|\frac{\sqrt{3}}{2}d\right|^2. \tag{58}$$

The mass eigenvalues are determined as

$$m_1^2=\frac{A+D}{2}\mp\frac{1}{2}\sqrt{(A-D)^2+4|B|^2}, \tag{59}$$

$$m_2^2=C, \tag{60}$$

$$m_3^2=\frac{A+D}{2}\pm\frac{1}{2}\sqrt{(A-D)^2+4|B|^2}, \tag{61}$$

where the upper and lower signs in these mass eigenvalues correspond to the normal hierarchy (NH) and the inverted hierarchy (IH). Next, we diagonalize the rotated mass matrices, Eqs. (53) and (54), with $U_{13}(\theta,\sigma)$ and $U_{13}^*(\theta+\frac{\pi}{2},\sigma)$ respectively:

$$U_{13}(\theta,\sigma)^\dagger\begin{pmatrix} A & 0 & B \\ 0 & C & 0 \\ B^* & 0 & D \end{pmatrix}U_{13}(\theta,\sigma)=\begin{pmatrix} m_1^2 & & \\ & m_2^2 & \\ & & m_3^2 \end{pmatrix}, \tag{62}$$

$$U_{13}\left(\theta+\frac{\pi}{2},\sigma\right)^{\rm T}\begin{pmatrix} D & 0 & -B^* \\ 0 & C & 0 \\ -B & 0 & A \end{pmatrix}U_{13}\left(\theta+\frac{\pi}{2},\sigma\right)^*$$

$$=\begin{pmatrix} m_1^2 & & \\ & m_2^2 & \\ & & m_3^2 \end{pmatrix}, \tag{63}$$

where θ and σ are determined as,

$$\tan2\theta=\frac{2|B|}{D-A}\ ,\ \sigma=-\varphi_B. \tag{64}$$

Finally, the other parameters ϕ_i are determined as follows,

$$\phi_1=\frac{1}{2}\left[\tan^{-1}\left[\frac{\left({\rm Im}[a]+{\rm Im}\left[c-\frac{d}{2}\right]\cos2\theta\right)\cos\sigma+\left({\rm Re}[a]\cos2\theta+{\rm Re}\left[c-\frac{d}{2}\right]\right)\sin\sigma-\frac{\sqrt{3}}{2}{\rm Im}[d]\sin2\theta}{\left({\rm Re}[a]+{\rm Re}\left[c-\frac{d}{2}\right]\cos2\theta\right)\cos\sigma-\left({\rm Im}[a]\cos2\theta+{\rm Im}\left[c-\frac{d}{2}\right]\right)\sin\sigma-\frac{\sqrt{3}}{2}{\rm Re}[d]\sin2\theta}\right]-\sigma\right], \tag{65}$$

$$\phi_2=\frac{1}{2}\tan^{-1}\left[\frac{{\rm Im}[a^2-(c^2-cd+d^2)]{\rm Re}[2d-c]-{\rm Re}[a^2-(c^2-cd+d^2)]{\rm Im}[2d-c]}{{\rm Re}[a^2-(c^2-cd+d^2)]{\rm Re}[2d-c]+{\rm Im}[a^2-(c^2-cd+d^2)]{\rm Im}[2d-c]}\right], \tag{66}$$

$$\phi_3=\frac{1}{2}\left[\tan^{-1}\left[\frac{\left({\rm Im}[a]-{\rm Im}\left[c-\frac{d}{2}\right]\cos2\theta\right)\cos\sigma-\left({\rm Re}[a]\cos2\theta-{\rm Re}\left[c-\frac{d}{2}\right]\right)\sin\sigma+\frac{\sqrt{3}}{2}{\rm Im}[d]\sin2\theta}{\left({\rm Re}[a]-{\rm Re}\left[c-\frac{d}{2}\right]\cos2\theta\right)\cos\sigma+\left({\rm Im}[a]\cos2\theta-{\rm Im}\left[c-\frac{d}{2}\right]\right)\sin\sigma+\frac{\sqrt{3}}{2}{\rm Re}[d]\sin2\theta}\right]+\sigma\right]. \tag{67}$$

1) There are six real parameters since b is written by using a,c,d.

We briefly explain the derivation of ϕ_i for the mass matrix $M_\nu^{\rm I}$. We first diagonalize $M_\nu^{\rm I}$ with the unitary matrices $U_{\rm TBM}$ and $U_{13}(\theta,\sigma)$ according to Eq. (48). However, the diagonalized neutrino mass matrix consists of complex elements. Then, the parameters ϕ_i are determined so that all the elements of the diagonalized matrix are real and positive.

4 Phenomenological aspects

We study the phenomenological aspects of this model and show the differences between the two types of vacua. The observables, such as mixing angles and CP violating phases, are described with the model parameters in different forms for the two types. In the following subsections, we discuss the relation between the observables and model parameters. The numerical analyses are also shown in this section.

4.1 Mixing angles and CP violating phases

In this subsection, we discuss the lepton mixing angles, CP violating phases and the effective mass for $0\nu\beta\beta$ decay. At first, we introduce the PDG parametrization of the PMNS matrix:

$$U_{\rm PMNS}^{\rm PDG}=\begin{pmatrix} c_{12}c_{13} & s_{12}c_{13} & s_{13}e^{-i\delta_{CP}} \\ -s_{12}c_{23}-c_{12}s_{23}s_{13}{\rm e}^{{\rm i}\delta_{CP}} & c_{12}c_{23}-s_{12}s_{23}s_{13}{\rm e}^{{\rm i}\delta_{CP}} & s_{23}c_{13} \\ s_{12}c_{23}-c_{12}c_{23}s_{13}{\rm e}^{{\rm i}\delta_{CP}} & -c_{12}s_{23}-s_{12}c_{23}s_{13}{\rm e}^{{\rm i}\delta_{CP}} & c_{23}c_{13} \end{pmatrix}\begin{pmatrix} {\rm e}^{{\rm i}\alpha} & & \\ & {\rm e}^{{\rm i}\beta} & \\ & & 1 \end{pmatrix}, \tag{68}$$

where s_{ij} and c_{ij} denote the lepton mixing angles $\sin\theta_{ij}$ and $\cos\theta_{ij}$, respectively. They are written in terms of the PMNS matrix elements:

$$\sin^2\theta_{12}=\frac{|U_{e2}|^2}{1-|U_{e3}|^2},\ \sin^2\theta_{23}=\frac{|U_{\mu3}|^2}{1-|U_{e3}|^2},\ \sin^2\theta_{13}=|U_{e3}|^2, \tag{69}$$

where $U_{\alpha i}$ denote the PMNS matrix elements. The Dirac CP violating phase δ_{CP} can be obtained with the Jarlskog invariant

$$\sin\delta_{CP}=\frac{J_{CP}}{s_{23}c_{23}s_{12}c_{12}s_{13}c_{13}^2}, \tag{70}$$

$$J_{CP}={\rm Im}\left[U_{e1}U_{\mu2}U_{\mu1}^*U_{e2}^*\right]. \tag{71}$$

In order to obtain these parameters from our model, we substitute the PMNS matrix elements in Eqs. (49) and (50). For the type I case, the matrix elements are given as follows:

$$U_{e1}=\frac{2}{\sqrt{6}}{\rm e}^{{\rm i}\phi_1}\cos\theta, \tag{72}$$

$$U_{e2}=U_{\mu2}=\frac{1}{\sqrt{3}}{\rm e}^{{\rm i}\phi_2}, \tag{73}$$

$$U_{e3}=\frac{2}{\sqrt{6}}e^{-i(\sigma-\phi_3)}\sin\theta, \tag{74}$$

$$U_{\mu1}=\left(-\frac{1}{\sqrt{6}}\cos\theta+\frac{1}{\sqrt{2}}{\rm e}^{{\rm i}\sigma}\sin\theta\right){\rm e}^{{\rm i}\phi_1}, \tag{75}$$

$$U_{\mu3}=\left(-\frac{1}{\sqrt{6}}e^{-i\sigma}\sin\theta-\frac{1}{\sqrt{2}}\cos\theta\right){\rm e}^{{\rm i}\phi_3}. \tag{76}$$

The mixing angles, Dirac CP violating phase and Majorana phases for both types are listed in Table 3.

Table 3. Mixing angles, Dirac CP phase and Majorana phases for the two types of vacua.

	Type I	Type II
$\sin^2\theta_{12}$	$\frac{1}{2+\cos2\theta}$	$\frac{1}{2-\cos2\theta}$
$\sin^2\theta_{23}$	$\frac{1}{2}\left(1+\frac{\sqrt{3}\sin2\theta}{2+\cos2\theta}\cos\sigma\right)$	$\frac{1}{2}\left(1-\frac{\sqrt{3}\sin2\theta}{2-\cos2\theta}\cos\sigma\right)$
$\sin^2\theta_{13}$	$\frac{1}{3}(1-\cos2\theta)$	$\frac{1}{3}(1+\cos2\theta)$
$\sin\delta_{CP}$	$-\frac{\sin2\theta}{\lvert\sin2\theta\rvert}\frac{(2+\cos2\theta)\sin\sigma}{\sqrt{(2+\cos2\theta)^2-3\sin^2 2\theta\cos^2\sigma}}$	$-\frac{\sin2\theta}{\lvert\sin2\theta\rvert}\frac{(2-\cos2\theta)\sin\sigma}{\sqrt{(2-\cos2\theta)^2-3\sin^2 2\theta\cos^2\sigma}}$
$\alpha+\delta_{CP}$	$\phi_1-\phi_3+\sigma$	$\phi_1-\phi_3+\sigma$
$\beta+\delta_{CP}$	$\phi_2-\phi_3+\sigma$	$\phi_2-\phi_3+\frac{\pi}{2}$

One can adopt either of the two types to predict the mixing angles and the Dirac CP violating phases, since both types give the same predictions. However, we note the following two facts. First, if one fixes $\cos2\theta\simeq1$ to obtain small $\sin^2\theta_{13}$ in type I, $\sin^2\theta_{13}$ in type II reaches 2/3, which is disfavored in the experiments. Second, as shown in Subsection 3.3, the model parameters θ, σ and ϕ_i are expressed in the same forms for the two types with a, b,

c and d of Eq. (27). Therefore, those parameters have common values for both types. Hence, the two types can not realize the experimental results simultaneously.

Next, we discuss the effective mass for $0\nu\beta\beta$ decay, $m_{ee}=\sum_i m_i U_{ei}^2$, and the Majorana phases, α and β. The effective mass is given as follows:

$$|m_{ee}^{\rm I}|=\frac{1}{3}\big|m_1(1+\cos2\theta)e^{2i\phi_1}+m_2e^{2i\phi_2} +m_3(1-\cos2\theta)e^{2i(\phi_3-\sigma)}\big|, \tag{77}$$

$$|m_{ee}^{\rm II}|=\frac{1}{3}\big|m_1(1-\cos2\theta)e^{2i(\phi_1+\sigma)}-m_2e^{2i\phi_2} +m_3(1+\cos2\theta)e^{2i\phi_3}\big|, \tag{78}$$

where the superscripts I and II denote the types of vacuum. Equivalently, one can rewrite Eqs. (77) and (78) as

$$|m_{ee}^{\rm I}|=\frac{1}{3}\big|m_1(1+\cos2\theta)e^{2i(\phi_1-\phi_3+\sigma)}+m_2e^{2i(\phi_2-\phi_3+\sigma)} +m_3(1-\cos2\theta)\big|, \tag{79}$$

$$|m_{ee}^{\rm II}|=\frac{1}{3}\big|m_1(1-\cos2\theta)e^{2i(\phi_1-\phi_3+\sigma)}-m_2e^{2i(\phi_2-\phi_3)} +m_3(1+\cos2\theta)\big|, \tag{80}$$

On the other hand, the effective mass in the PDG parametrization is written as

$$|m_{ee}|=\big|m_1c_{13}^2c_{12}^2e^{2i(\alpha+\delta_{CP})}+m_2c_{13}^2s_{12}^2e^{2i(\beta+\delta_{CP})}+m_3s_{13}^2\big|. \tag{81}$$

One can obtain the Majorana CP violating phases α and β by comparing Eqs (79)-(81),

$$\text{(Type I)}\quad \alpha+\delta_{CP}=\phi_1-\phi_3+\sigma\ ,\quad \beta+\delta_{CP}=\phi_2-\phi_3+\sigma, \tag{82}$$

$$\text{(Type II)}\quad \alpha+\delta_{CP}=\phi_1-\phi_3+\sigma\ ,\quad \beta+\delta_{CP}=\phi_2-\phi_3+\frac{\pi}{2}. \tag{83}$$

4.2 Numerical analysis

In this subsection, we show numerical analysis to find the difference between two types. We use recent experimental results with 3σ range [22], as summarized in Table 4.

Table 4. The experimental data for the mass squared differences and mixing angles with 3σ range [22].

	normal hierarchy (NH)	inverted hierarchy (IH)
$\Delta m_{21}^2/\text{eV}^2$	$(7.03\sim8.09)\times10^{-5}$	$(7.03\sim8.09)\times10^{-5}$
$\Delta m_{31}^2/\text{eV}^2$	$(2.407\sim2.643)\times10^{-3}$	$-(2.565\sim2.318)\times10^{-3}$
$\sin^2\theta_{12}$	$0.271\sim0.345$	$0.271\sim0.345$
$\sin^2\theta_{23}$	$0.385\sim0.635$	$0.393\sim0.640$
$\sin^2\theta_{13}$	$0.01934\sim0.02392$	$0.01953\sim0.02408$

As we have shown in the previous subsection, the mixing angles and Dirac CP phase are expressed in terms of the model parameters θ and σ in different forms for the two types.

The experimental data for $\sin^2\theta_{13}$ in Table 4 is realized by the following value of θ with NH or IH:

$$\text{Type I;}\ \ 9.81^\circ\leqslant|\theta|\leqslant10.9^\circ\ \text{(NH)},\ 9.86^\circ\leqslant|\theta|\leqslant11.0^\circ\ \text{(IH)}, \tag{84}$$

$$\text{Type II;}\ \ 79.1^\circ\leqslant|\theta|\leqslant80.2^\circ\ \text{(NH)},\ 79.0^\circ\leqslant|\theta|\leqslant80.1^\circ\ \text{(IH)}. \tag{85}$$

The value of σ is allowed in $-180^\circ\leqslant\sigma\leqslant180^\circ$ for both of the two types, since the error of $\sin^2\theta_{23}$ from the experiments is large.

Next, we discuss the parameters ϕ_i in the expressions of the Majorana phases of Eqs. (82) and (83). The effective mass $|m_{ee}|$ in Eq. (81) depends on the two combinations of Dirac and Majorana phases, $2(\alpha+\delta_{CP})$ and $2(\beta+\delta_{CP})$. If we determine both $|m_{ee}|$ and the lightest neutrino mass, we obtain the constraints on these two combinations. In order to find how the numerical constraints on ϕ_i are different in the two types, we consider a specific situation. As an example, we assume that $|m_{ee}|$ is predicted in the region as shown in Fig. 3. We note that the lightest neutrino mass is constrained from the cosmological upper bound for the neutrino mass sum, $\sum_i m_i<0.16$ eV [23]. This plot is obtained when the Dirac and Majorana phases are randomly chosen from the region A1 in Fig. 2,

$$0<\alpha+\delta_{CP}<\pi/4\ ,\ 0<\beta+\delta_{CP}<\pi/4. \tag{86}$$

In this situation, the phase differences $\phi_1-\phi_3$ and $\phi_2-\phi_3$ for one type can be distinguished from those for the other type. The constraints on the phase differences are shown in Fig. 4. For type I, the phase difference $\phi_2-\phi_3$ is proportional to $\phi_1-\phi_3$. However, for type II, $\phi_2-\phi_3$ is independent of the value of $\phi_1-\phi_3$ because σ is absent in the expression of $\phi_2-\phi_3$ in Eq. (83).

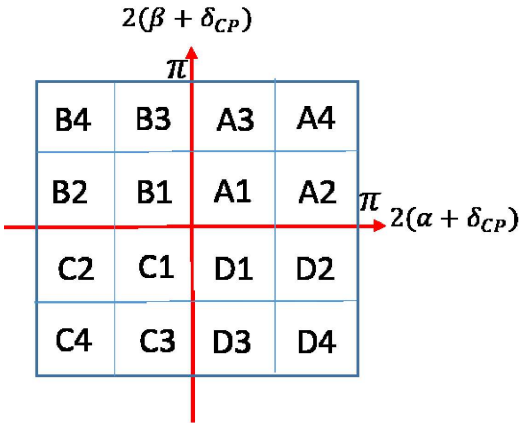

Fig. 2. (color online) 16 divided regions for $2(\alpha+\delta_{CP})$ and $2(\beta+\delta_{CP})$.

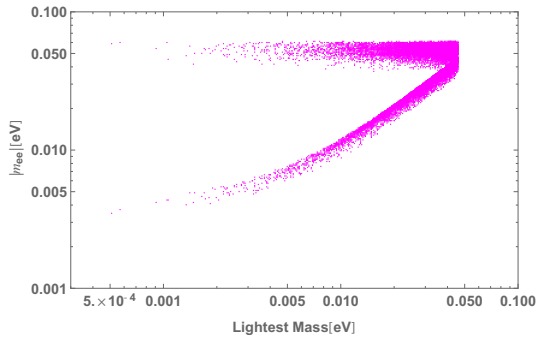

Fig. 3. (color online) The prediction of effective mass for $0\nu\beta\beta$ decay in region A1 of Fig. 2. The upper region corresponds to the IH case , while the lower one corresponds to the NH case.

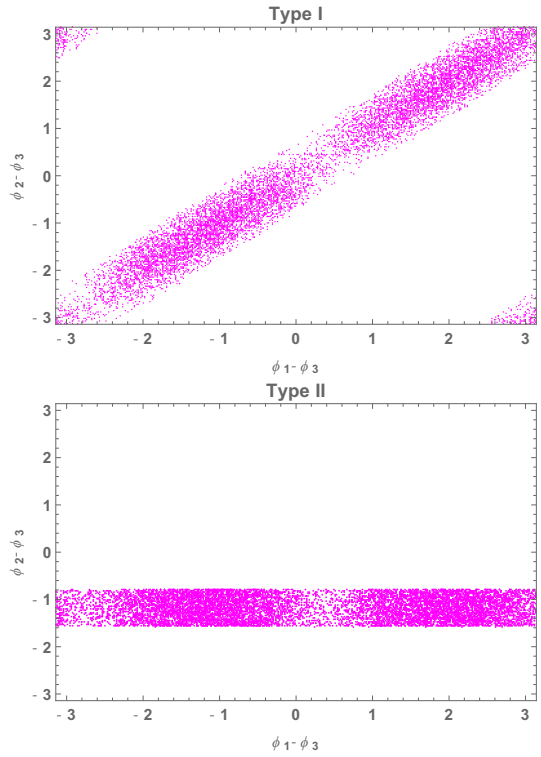

Fig. 4. (color online) The allowed regions of the model parameters, $\phi_1-\phi_3$ and $\phi_2-\phi_3$ for both types of vacua. These plots correspond to region A1 of Fig. 2.

5 Summary

We have studied phenomenological aspects of a supersymmetric model with $A_4\times Z_3$ symmetry. We found 24 degenerate vacua at the 24 minima of the scalar potential. Then, we discussed the relations among the 24 different vacua and classified them into two types. Both types consist of 12 vacua which are related to each other by transformations of A_4. We proved that the 12 vacua are equivalent and lead to the same physical consequences. However, we found that we obtain different physical consequences from the vacua of different types. Therefore, we analyzed the two types of vacua to find the different phenomenological consequences of the two types. In particular, we investigated observables such as mixing angles, Dirac CP phase, Majorana phases and effective mass for $0\nu\beta\beta$ decay.

These observables are expressed in terms of the model parameters θ, σ and ϕ_i. The angle θ and phase σ are determined by the deviation from the tri-bimaximal mixing matrix. The two types lead to different expressions for the mixing angles and Dirac CP violating phase in terms of θ and σ. Therefore, one should take different model parameters in each type in order to realize the experimental results. Although one can adopt both of the two types to predict the observable parameters, the two types cannot realize the current experimental data simultaneously. The Majorana phases α and β are parametrized in the different expressions for each type by the model parameters ϕ_i in addition to θ and σ. In order to find numerical differences between the two types of Majorana phase, we considered the specific situation where the lightest mass and effective mass for the $0\nu\beta\beta$ decay are determined in a certain region. We showed the allowed regions of the phase differences, $\phi_1-\phi_3$ and $\phi_2-\phi_3$. The regions are quite different for the two types: the phase differences for type I are proportional to each other, while those for type II are not.

The VEVs η_m and $\lambda_n^{\pm}$ transfer to the different VEVs by transformations of A_4. However, the transformations for η_m and $\lambda_n^{\pm}$ are closed differently since they have the Z_3 and Z_2 residual symmetries from A_4 respectively. We have pointed out that some combinations of the VEVs can lead to different physical consequences. When we consider models with two or more flavons, we should take account of the combination of VEVs.

Appendix A

Multiplication rule of A_4 group

In this appendix, we show the multiplication of the A_4 group. The multiplication rule of the triplets is written as follows;

$$\begin{pmatrix} a_1 \\ a_2 \\ a_3 \end{pmatrix}_{\mathbf{3}} \otimes \begin{pmatrix} b_1 \\ b_2 \\ b_3 \end{pmatrix}_{\mathbf{3}} = (a_1b_1+a_2b_3+a_3b_2)_{\mathbf{1}} \oplus (a_3b_3+a_1b_2+a_2b_1)_{\mathbf{1'}} \oplus (a_2b_2+a_1b_3+a_3b_1)_{\mathbf{1''}} \oplus \frac{1}{3}\begin{pmatrix} 2a_1b_1-a_2b_3-a_3b_2 \\ 2a_3b_3-a_1b_2-a_2b_1 \\ 2a_2b_2-a_1b_3-a_3b_1 \end{pmatrix}_{\mathbf{3}} \oplus \frac{1}{2}\begin{pmatrix} a_2b_3-a_3b_2 \\ a_1b_2-a_2b_1 \\ a_3b_1-a_1b_3 \end{pmatrix}_{\mathbf{3}}, \tag{A1}$$

while that for singlets is,

$$\mathbf{1'} \otimes \mathbf{1''} = \mathbf{1}. \tag{A2}$$

In order to derive the A_4 invariant superpotential in Eq. (1), we have used the multiplication rules. Their derivation is shown in the reviews in Refs. [1–4].

References

1 H. Ishimori, T. Kobayashi, H. Ohki, Y. Shimizu, H. Okada, and M. Tanimoto, Prog. Theor. Phys. Suppl., **183**: 1 (2010) [arXiv:1003.3552 [hep-th]]
2 H. Ishimori, T. Kobayashi, H. Ohki, H. Okada, Y. Shimizu, and M. Tanimoto, Lect. Notes Phys., **858**: 1 (2012)
3 H. Ishimori, T. Kobayashi, Y. Shimizu, H. Ohki, H. Okada, and M. Tanimoto, Fortsch. Phys., **61**: 441 (2013)
4 S. F. King, A. Merle, S. Morisi, Y. Shimizu, and M. Tanimoto, New J. Phys., **16**: 045018 (2014) [arXiv:1402.4271 [hep-ph]]
5 F. P. An et al (Daya Bay Collaboration), Phys. Rev. Lett., **108**: 171803 (2012) [arXiv:1203.1669 [hep-ex]]
6 J. K. Ahn et al (RENO Collaboration), Phys. Rev. Lett., **108**: 191802 (2012) [arXiv:1204.0626 [hep-ex]]
7 Y. Abe et al (Double Chooz Collaboration), Phys. Lett. B, **735**: 51 (2014) [arXiv:1401.5981 [hep-ex]]
8 Y. Shimizu, M. Tanimoto, and A. Watanabe, Prog. Theor. Phys., **126**: 81 (2011) [arXiv:1105.2929 [hep-ph]]
9 K. Abe et al (T2K Collaboration), Phys. Rev. Lett., **112**: 061802 (2014) [arXiv:1311.4750 [hep-ex]]
10 P. Adamson et al (NOvA Collaboration), Phys. Rev. Lett., **116**(15): 151806 (2016) [arXiv:1601.05022 [hep-ex]]
11 A. Gando et al (KamLAND-Zen Collaboration), Phys. Rev. Lett., **117**(8): 082503 (2016); Addendum: [Phys. Rev. Lett., **117**(10): 109903 (2016)] [arXiv:1605.02889 [hep-ex]]
12 P. F. Harrison, D. H. Perkins, and W. G. Scott, Phys. Lett. B, **530**: 167 (2002) [hep-ph/0202074]
13 P. F. Harrison and W. G. Scott, Phys. Lett. B, **535**: 163 (2002) [hep-ph/0203209]
14 G. Altarelli and F. Feruglio, Nucl. Phys. B, **720**: 64 (2005) [hep-ph/0504165]
15 G. Altarelli and F. Feruglio, Nucl. Phys. B, **741**: 215 (2006) [hep-ph/0512103]
16 N. Haba, A. Watanabe, and K. Yoshioka, Phys. Rev. Lett., **97**: 041601 (2006) [hep-ph/0603116]
17 H. Ishimori, Y. Shimizu, M. Tanimoto, and A. Watanabe, Phys. Rev. D, **83**: 033004 (2011) [arXiv:1010.3805 [hep-ph]]
18 W. Grimus and L. Lavoura, JHEP, **0809**: 106 (2008) [arXiv:0809.0226 [hep-ph]]
19 P. Minkowski, Phys. Rev. B, **67**: 421 (1977)
20 T. Yanagida, *Horizontal Symmetry And Masses Of Neutrinos*, in *Workshop on the Unified Theories and the Baryon Number in the Universe*, Tsukuba, Japan, February 13-14, 1979, KEK-79-18. EDS. O. Sawada, A. Sugamoto, Conf. Proc. C, **7902131**: 95 (1979)
21 M. Gell-Mann, P. Ramond, and R. Slansky, Conf. Proc. C, **790927**: 315 (1979) [arXiv:1306.4669 [hep-th]] "Supergravity", EDS. P. van Nieuwenhuizen, D. Z. Freedman, Proceedings, Workshop At Stony Brook, 27-29 September 1979, Amsterdam, (Netherlands: North-holland, 1979) 341p
22 I. Esteban, M. C. Gonzalez-Garcia, M. Maltoni, I. Martinez-Soler, and T. Schwetz, JHEP, **1701**: 087 (2017) [arXiv:1611.01514 [hep-ph]]
23 S. Alam et al (BOSS Collaboration), arXiv:1607.03155 [astro-ph.CO]